Biochemical and Biophysical Research Communications 443 (2014) 783–788

Contents lists available at ScienceDirect

Biochemical and Biophysical Research Communications

journal homepage: www.elsevier.com/locate/ybbrc

Crystal structure of (R)-3-hydroxybutyryl-CoA dehydrogenase PhaB from *Ralstonia eutropha*

Jieun Kim [a], Jeong Ho Chang [b], Eun-Jung Kim [a], Kyung-Jin Kim [a,*]

[a] Structural and Molecular Biology Laboratory, School of Life Sciences and Biotechnology, Kyungpook National University, Daehak-ro 80, Buk-ku, Daegu 702-701, Republic of Korea
[b] Department of Biology, Teachers College, Kyungpook National University, Daehak-ro 80, Buk-ku, Daegu 702-701, Republic of Korea

ARTICLE INFO

Article history:
Received 24 October 2013
Available online 6 November 2013

Keywords:
(R)-3-hydroxybutyryl-CoA dehydrogenase
Polyhydroxyalkanoate
Ralstonia eutropha
Crystal structure

ABSTRACT

(R)-3-hydroxybutyryl-CoA dehydrogenase PhaB from *Ralstonia eutropha* H16 (*Re*PhaB) is an enzyme that catalyzes the NADPH-dependent reduction of acetoacetyl-CoA, an intermediate of polyhydroxyalkanoates (PHA) synthetic pathways. Polymeric PHA is used to make bioplastics, implant biomaterials, and biofuels. Here, we report the crystal structures of *Re*PhaB apoenzyme and in complex with either $NADP^+$ or acetoacetyl-CoA, which provide the catalytic mechanism of the protein. *Re*PhaB contains a Rossmann fold and a Clamp domain for binding of $NADP^+$ and acetoacetyl-CoA, respectively. The $NADP^+$-bound form of *Re*PhaB structure reveals that the protein has a unique cofactor binding mode. Interestingly, in the *Re*PhaB structure in complex with acetoacetyl-CoA, the conformation of the Clamp domain, especially the Clamp-lid, undergoes a large structural change about 4.6 Å leading to formation of the substrate pocket. These structural observations, along with the biochemical experiments, suggest that movement of the Clamp-lid enables the substrate binding and ensures the acetoacetyl moiety is located near to the nicotinamide ring of $NADP^+$.

1. Introduction

In order to store carbons as their energy source, bacteria produce the linear polyesters polyhydroxyalkanoates (PHAs) via fermentation of either sugars or lipids [1]. Over 150 PHA monomers with different thermal and mechanical properties have been reported so far [2]. Considerable research has been focused on understanding the mechanism of PHA biosynthesis, and numerous advances have been made using molecular genetic analysis [3–5].

Over the past 10 years, efforts have been made to elucidate how best to utilize PHAs [6]. PHAs can be used to produce bioplastics, fine chemicals, implant biomaterials, medicines, and biofuels [7–10]. Petroleum is a widely used non-sustainable resource, that is being rapidly depleted and, therefore, alternate resources are required. Biosynthesis of PHAs is conducted by microorganisms grown in an aqueous solution containing sustainable resources such as starch, glucose, sucrose, fatty acids, and nutrients in waste water at 30–37 °C and atmospheric pressure. Therefore, PHAs are considered sustainable, environmentally friendly plastics [11,12].

Various mechanisms of PHA production have been reported [2,13,14]. Biosynthetic production of PHAs leads to a much higher molecular weight than chemical methods. *Ralstonia eutropha* is the representative bacterial strain used for PHA biosynthesis, but several other bacteria, such as *Aeromonas hydrophila*, *Pseudomonas stutzeri* [15] and *Pseudomonas oleovorans* have the same biosynthetic pathways to produce PHAs [5,16–19]. Three key enzymes β-ketothiolase, NADPH-dependent acetoacetyl-CoA reductase, and PHA synthase (encoded by genes corresponding to *phaA*, *phaB*, and *phaC*, respectively) are involved in PHA-biosynthesis [20].

The biosynthetic pathway of PHAs in *R. eutropha* was engineered in *Escherichia coli*, and is roughly divided to two stages monomer synthesis and polymerization [21]. Two enzymes are involved in synthesis of the monomer (R)-3-hydroxybutyryl-CoA. PhaA initially combines two acetyl-CoAs producing acetoacetyl-CoA which is the substrate of PhaB. The acetoacetyl-CoA is then converted to the monomer of PHAs by PhaB. The polymerization step is catalyzed by PhaC to generate biodegradable plastics that can be produced at 50% dry cell weight of the maximum theoretical yield [20]. Although the rate of PhaA-dependent C–C bond formation is low, the process is strongly driven by depletion of the PHA monomer by PhaC *in vivo*, which allows its physical sequestration as a polymer [10,22]. Therefore, PhaA and PhaB could be capable of supporting a high rate PHA production if a similar irreversible physical step, such as the release of free CoAs or secretion of the *n*-butanol product from the cell, occurs in a later reaction step [23].

Given the potential role of PHA as a bioplastic, the ultimate goal is to improve the efficiency of each step of its biosynthesis. Although several biochemical studies have been performed to assess the roles of PhaA, PhaB, and PhaC in the biosynthetic

* Corresponding author. Fax: +82 53 955 5522.
E-mail address: kkim@knu.ac.kr (K.-J. Kim).

0006-291X/$ - see front matter © 2013 Elsevier Inc. All rights reserved.
http://dx.doi.org/10.1016/j.bbrc.2013.10.150

pathways, the structural information of these enzymes is limited. Among the three enzymes, PhaB is responsible to producing the monomer of PHA in an NADPH-dependent manner, so it is directly linked to the efficiency of PHA biosynthesis. In this sense, structural data of PhaB could provide key details for improving its efficiency in a molecular level. In this study, we report the crystal structure of PhaB from *R. eutropha* H16 as an apoenzyme and in complexes with either a cofactor or a substrate. We identified the critical structural factors for PhaB recognition of acetoacetyl-CoA, which could provide a platform for improving the enzyme's efficiency.

2. Materials and methods

2.1. Cloning, expression, and purification

The *Re*PhaB coding gene was amplified from the *R. eutropha* H16 chromosome by a polymerase chain reaction (PCR). Using the BamHI and HindIII restriction enzymes, the PCR product was then subcloned into $pP_{RO}EX$ HTa (Invitrogen) with 6xHis at the N-terminus and a recombinant TEV protease (rTEV) cleavage site. The resulting expression vector $pP_{RO}EX$ HTa:*RePhaB* was transformed into *E. coli* B834 strain and the cells were grown in an LB medium containing 100 μM of ampicillin at 37 °C. After induction with 0.5 mM Isopropyl β-D-1-thiogalactopyranoside (IPTG), the cells were further grown for 20 h at 18 °C, and harvested by centrifugation at 4000*g* at 4 °C. Cell pellet was resuspended in ice-cold buffer A (40 mM Tris–HCl, pH 8.0) and disrupted by ultrasonication. The cell debris was removed by centrifugation at 13,500*g* for 25 min, and lysate was bound to Ni-NTA agarose (QIAGEN). After washing with buffer A containing 20 mM imidazole, the bound proteins were eluted with 300 mM imidazole in buffer A. The resulting recombinant protein had extra amino acids of Gly-Ala in front of the first methionine. Finally the trace amount of contaminants was removed by a size exclusion chromatography using a Superdex 200 prep grade (320 ml, GE Healthcare) equilibrated with buffer A containing 5 mM β-mercaptoethanol. The protein was eluted with a molecular weight of ~120 kDa, indicating the *Re*PhaB protein with molecular weight of 29 kDa forms a tetrameric structure. All purification experiments were performed at 4 °C. The degree of protein purification was confirmed by SDS–PAGE. The purified protein was concentrated to 20 mg/ml in 40 mM Tris–HCl, pH 8.0, 5 mM β-mercaptoethanol.

2.2. Crystallization and data collection

Crystallization of the purified protein was initially performed with commercially available sparse-matrix screens from Hampton Research and Emerald BioSystems using the hanging-drop vapor-diffusion method at 295 K. Each experiment consisted of mixing 1.2 μl protein solution (20 mg/ml in 20 mM Tris–HCl pH 8.0 and 5 mM β-mercaptoethanol) with 1.2 μl reservoir solution and then equilibrating it against 0.5 ml of the reservoir solution. *Re*PhaB crystals were observed from several crystallization screening conditions. After several steps that improved the crystallization process using the hanging-drop vapor-diffusion method, crystals of the best quality appeared in 3 days and reached their maximal dimensions of approximately 0.2 × 0.2 × 0.4 mm using reservoir solution containing 13% ethanol, 0.1 M Citrate, pH 7.0 and 0.2 M lithium sulfate.

The crystals were transferred to a cryoprotectant solution containing 13% ethanol, 0.1 M Citrate, pH 7.0 and 0.2 M lithium sulfate and 30% (v/v) glycerol, fished out with a loop larger than the crystals and flash-frozen by immersion in liquid nitrogen at 100 K. The data were collected to a resolution of 1.65 Å at 7 A beamline of the Pohang Accelerator Laboratory (PAL, Pohang, Korea) using a Quantum 270 CCD detector (ADSC, USA). All data were indexed, integrated and scaled together using the HKL2000 software package [24]. The crystals of both the *Re*PhaB apo and the *Re*PhaB-$NADP^+$ complex belonged to the space group $C222_1$, while the *Re*PhaB-acetoacetyl-CoA complex belonged the space group $P42_12$. Assuming that an asymmetric unit contains four molecules

Table 1
Data collection and refinement statistics.

	Apo	Complex with $NADP^+$	Complex with acetoacetyl-CoA
Data collection			
Space group	$C222_1$	$C222_1$	$P42_12$
Cell dimensions			
a, *b*, *c* (Å)	87.91, 94.34, 137.26	87.67, 94.73, 137.28	138.96, 138.96, 70.63
αβγ (°)	90.00, 90.00, 90.00	90.00, 90.00, 90.00	90.00, 90.00, 90.00
Resolution (Å)	50.00–1.65 (1.68–1.65)*	50.00–2.15 (2.03–2.15)	50.00–1.77 (1.80–1.77)
R_{sym} or R_{merge}	5.9 (24.9)	10.2 (30.5)	7.6 (27.3)
$I/\sigma I$	30.0 (3.0)	28.2 (12.7)	93.3 (24.2)
Completeness (%)	87.2 (81.9)	87.9 (92.8)	99.9 (100.0)
Redundancy	6.8 (3.1)	13.1 (13.6)	26.9 (26.1)
Refinement			
Resolution (Å)	32.18–1.65	29.15–2.15	28.69–1.77
No. reflections	56,817	26,249	64,053
R_{work}/R_{free}	24.5/29.2	24.0/31.7	15.1/17.4
No. atoms	3983	4069	4286
Protein	3672	3682	3710
Ligand/ion	–	96	156
Water	311	291	420
B-factors	23.82	33.74	23.33
Protein	22.55	32.70	15.66
Ligand/ion	–	69.05	42.75
Water	30.00	41.98	30.00
R.m.s. deviations			
Bond lengths (Å)	0.019	0.019	0.023
Bond angles (°)	1.872	1.967	2.198

[AU: Equations defining various *R*-values are standard and hence are no longer defined in the footnotes.]
[AU: Ramachandran statistics should be in Methods section at the end of Refinement subsection.]
[AU: Wavelength of data collection, temperature and beamline should all be in Methods section.]
* Number of xtals for each structure should be noted in footnote. Values in parentheses are for highest-resolution shell.

of *Re*PhaB, the crystal volume per unit of protein mass is 2.78 $Å^3$ Da^{-1}, which means the solvent content is approximately 55.7%.

2.3. Structure determination

The structure was determined by molecular replacement with the CCP4 version of MOLREP [25] using the structure of *E. coli* FabG (Protein Data Bank [PDB] code 1Q7B) as a search model. Model building was performed manually using the program WinCoot [26] and the refinement was performed with CCP4 refmac5 [27] and CNS [28]. For obtaining the cofactor and the substrate complex structures, we soaked either 100 mM $NADP^+$ or 100 mM acetoacetyl-CoA to the apo crystals for 1 h. The data statistics are summarized in Table 1. The refined *Re*PhaB models and structure factors were deposited in the Protein Data Bank as the PDB ID 4N5L, 4N5M and 4N5N for the apo, acetoacetyl-CoA complex and $NADP^+$ complex, respectively.

2.4. Site-directed mutagenesis and activity assay

Site-specific mutations were created with the QuikChange kit (stratagene), and sequencing was performed to confirm correct incorporation of the mutations. The mutant proteins were purified as same as the wild type. Enzyme activities of wild type and mutant proteins were measured by monitoring the change of $NADP^+$ absorbance at 340 nm. The reaction mixture (1 ml) contained 100 mM MOPS, pH 7.0, 5 mM β-mercaptoethanol, 0.2 mM NADPH, and 0.2 mM acetoacetyl-CoA. For each reaction 1 μg of wild-type or mutant *Re*PhaB protein was added to start the reaction, and the decrease of absorbance at 340 nm was monitored at room temperature for 3 min.

3. Results and discussion

3.1. Overall structure of RePhaB

To address the structural basis for the catalytic mechanism of NADPH-dependent PhaB from *R. eutropha*, we determined the crystal structures of *Re*PhaB in both apo and cofactor/substrate complex forms. Although two *Re*PhaB molecules are present in an asymmetric unit, the tetrameric structure of *Re*PhaB can easily be generated by applying the crystallographic $C222_1$ symmetry (Fig. 1A and B), which is consistent with the size-exclusion chromatography data (data not shown). The fan shaped tetrameric structure contains one each of two active sites on the front and back with twofold symmetries. There are two types of dimerization interface for the formation of a tetramer. One interface is formed

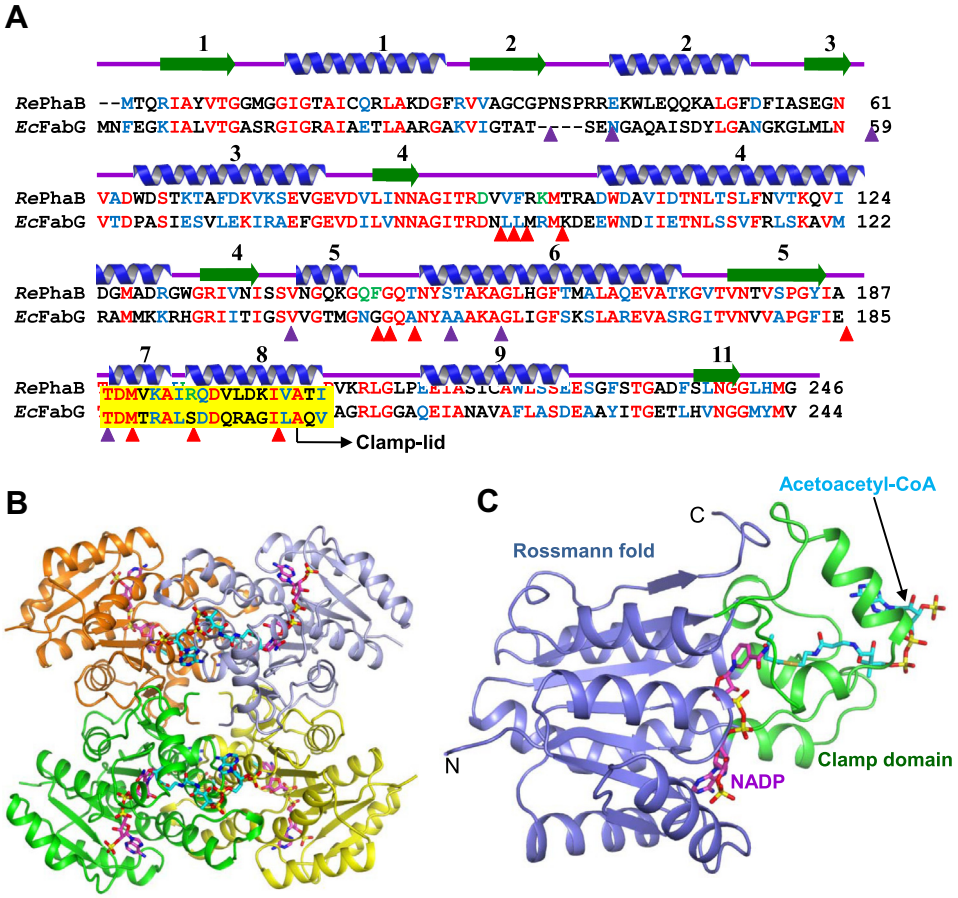

Fig. 1. Crystal structure of *Re*PhaB. (A) Amino acid sequence alignment of *Re*PhaB and *Ec*FabG. Secondary structure elements are drawn on the basis of *Re*PhaB structure and shown with a green-colored arrow (β-sheet) and blue-colored helix (α-helix). The "Clamp-lid domain" is shown in yellow color box. Residues involved in $NADP^+$ and acetoacetyl-CoA binding are indicated by purple- and red-colored triangles, respectively. *Re*PhaB and *Ec*FabG are representations of PhaB and FabG from *R. eutropha* and *E. coli*, respectively. (B) Tetrameric structure of *Re*PhaB. The tetrameric structure is shown as a ribbon diagram showing in orange, light blue, green and yellow colors. The bound ligands $NADP^+$ and acetoacetyl-CoA are shown in magenta and cyan colors, respectively. (C) Monomeric structure of *Re*PhaB. A monomeric protein is shown as a ribbon representation in which the Rossmann fold and the Clamp domain are distinguished with light blue and green colors, respectively. The bound $NADP^+$ and acetoacetyl-CoA are distinguished with magenta and cyan colors, respectively, and labeled appropriately. (For interpretation of the references to colour in this figure legend, the reader is referred to the web version of this article.)

between the β7 strands from each monomer, which results in a formation of a long β-sheet with 14 β-strands. The other interface is located between helices α4, α5 and α4′, α5′, which together form a 4-helical bundle through hydrophobic interactions.

The monomer contains a typical Rossmann fold structure, with a twisted, parallel β-sheet composed of seven β-strands flanked on both sides by a total of eight α helices (Fig. 1C). The core of the structure is composed of two right-handed βαβαβ motifs that are connected by helix α3. The overall structure of *Re*PhaB is similar to that of *E. coli* FabG which is a 3-oxoacyl-[acyl-carrier-protein] reductase except for a few substantial conformational differences at the substrate binding site that are discussed later. Interestingly, the two helices α4 and α6 are extended from the Rossmann fold so they generate a deep cleft together with the segment consisting of helix α7, loop α7-α8 and helix α8. Because the overall shape of the protruding segments looks like a clamp, we named it the Clamp domain. Additionally, hereafter we will refer to the segment α7, α7-α8 and α8 as the Clamp-lid, and the α4, partial β4-α4, α5-α6 and α6 segment as the Clamp-base.

3.2. RePhaB-cofactor complex structure

We determined the 2.15 Å resolution structure of *Re*PhaB in complex with $NADP^+$ cofactor. The overall structure of the $NADP^+$ complex is almost identical to the apoenzyme structure with a root-mean-square deviation of <0.3 Å. As expected, the $NADP^+$ cofactor is bound to the Rossmann fold as typically shown in other structures. In addition, the 3′-phosphorylated adenosine moiety of the $NADP^+$ is somewhat exposed at the surface, whereas the nicotinamide ribose moiety is buried by the Clamp domain so it is located in the deep cleft (Fig. 1C). The part of the enzyme that binds to $NADP^+$ is composed of five loops; β1–α1, β2–α2, partial β4–α4, β5–α5 and β6–α7. No interaction with the Clamp domain was found. The nicotinamide ring is positioned in an inner pocket which is the junction between the Rossmann fold and the Clamp domain, whereas the 3′-phosphate and adenine face outward.

$NADP^+$ is bound to the enzyme mainly through hydrogen bonds. The nicotinamide moiety interacts with the main chains of Gly184 and Ile186 as well as the side chain (OG1) of Thr188 (Fig. 2A). The dinucleotide moiety is stabilized by the main chains of Gly13, Gly14 and Asn88 and the side chains of Arg40 (NH2), Lys157 (NZ) and Tyr153 (OH). The adenine and the 3′-phosphate interact with the main chains of Gly35 and Gly60 and the side chains of Ser38 (OG), Arg40 (NH2) and Asn61 (OD1).

Although the overall binding mode of *Re*PhaB is similar to that of *E. coli*, there are also several differences [29]. First, the conformation of $NADP^+$ is slightly more extended in the *Re*PHaB protein than in the *Ec*FabG complex (Fig. 2B). Second, the binding of the 3′-phosphorylated adenosine moiety is clearly different. The conformation of β2–α2 that interacts with the adenine is more open in the *Re*PhaB, whereas the equivalent loop in *Ec*FabG is largely shifted towards the adenine. Third, the loop β1–α1 in *Re*PhaB interacts with the diphosphate groups of $NADP^+$, whereas the equivalent region of *Ec*FabG interacts with the α-phosphate and 3′-phosphate. Finally, the overall charge distribution of the $NADP^+$ binding pocket is different. In *Re*PhaB, it is mostly positively charged, whereas in *Ec*FabG it is less positive and rather somewhat hydrophobic.

3.3. Clamp-lid movement of the RePhaB-substrate complex

In contrast to $NADP^+$ binding, the substrate acetoacetyl-CoA is bound to the Clamp domain (Fig. 1C). The 3′-phosphate adenosine moiety is exposed at the surface, whereas the acetoacetyl group is located in the vicinity of the nicotinamide which acts as an electron donor for the reaction. Interestingly, conformation of the

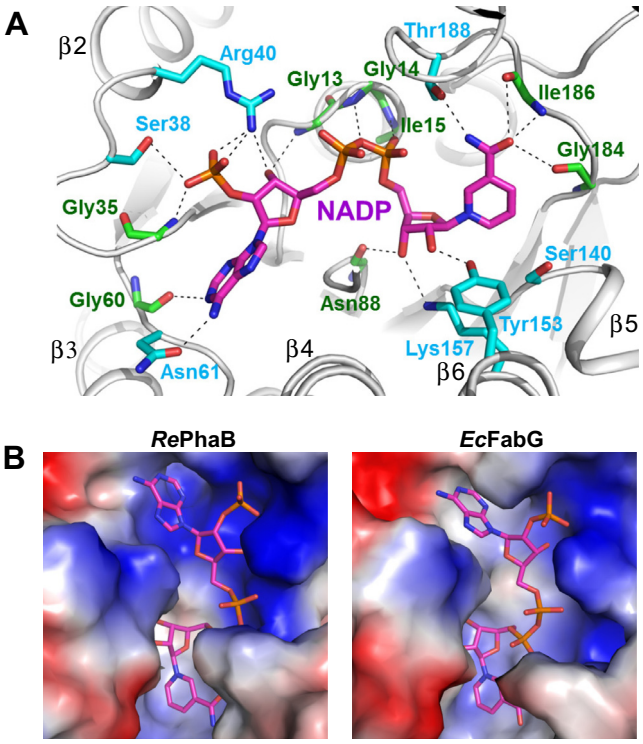

Fig. 2. The $NADP^+$ binding mode of *Re*PhaB. (A) Stabilization of $NADP^+$. The bound $NADP^+$ cofactor is presented in the stick model with magenta color and labeled appropriately. Side chains and main chains of the residues involved in $NADP^+$ binding are shown in cyan and green colors, respectively. Hydrogen bonds involved in the stabilization of $NADP^+$ are shown with black dotted-lines. (B) Comparison of $NADP^+$ binding between *Re*PhaB and *Ec*FabG. The *Re*PhaB (left) and *Ec*FabG (right; PDB code 1Q7B) structures were presented as surface electrostatic presentation, and shown with the same orientation. The $NADP^+$ cofactors are presented in the stick model with magenta color. (For interpretation of the references to colour in this figure legend, the reader is referred to the web version of this article.)

Clamp domain, especially the Clamp-lid, undergoes structural change about 4.6 Å toward the acetoacetyl-CoA compared to that of the $NADP^+$ complex (Fig. 3A). As discussed previously, compared with the apoenzyme structure, the binding of $NADP^+$ does not show any change on the Clamp domain. The structure clearly shows that if the Clamp-lid does not move inward, the acetoacetyl-CoA could not be tightly associated with the protein. Furthermore, since $NADP^+$ binds to a region of the enzyme separate to that of the Clamp domain, it is not affected by structural change. Therefore, the open-closed conformation of the Clamp-lid is responsible for substrate binding.

While $NADP^+$ interacts extensively by hydrogen bonding with residues in the cleft of *Re*PhaB, acetoacetyl-CoA is bound less stringently. The two carbonyl groups of the acetoacetyl moiety are bound via hydrogen bonds to the main chain of residue Gly184 and the nitrogen atom of the Q150 side chain (Fig. 3B). The pantotheine group is stabilized via hydrogen bonds to the side chains of residues Asp94, Gln147, Gln150 and Tyr185, and via Van der Waals interactions with Val 95, Val96 and Tyr185. The Tyr185 residue is also stabilized by Van der Waals interaction with Ile202. Met190 stabilizes part of the acetoacetyl group and the β-mercaptoethanolamine moiety. The two phosphate groups in the 3′-phosphate adenosine moiety are bound to the NH1 and NH2 groups of the Arg195 residue, and there is a water-mediated interaction between β-phosphate and Lys99. Additionally, the adenine is stably positioned by stacking with the Phe148 residue. The 3′-phosphate is shown to be hydrogen bonded to the main chain of Met1 only one molecule of the dimer. This could be an artifact caused by crystal packing and might not be biologically relevant.

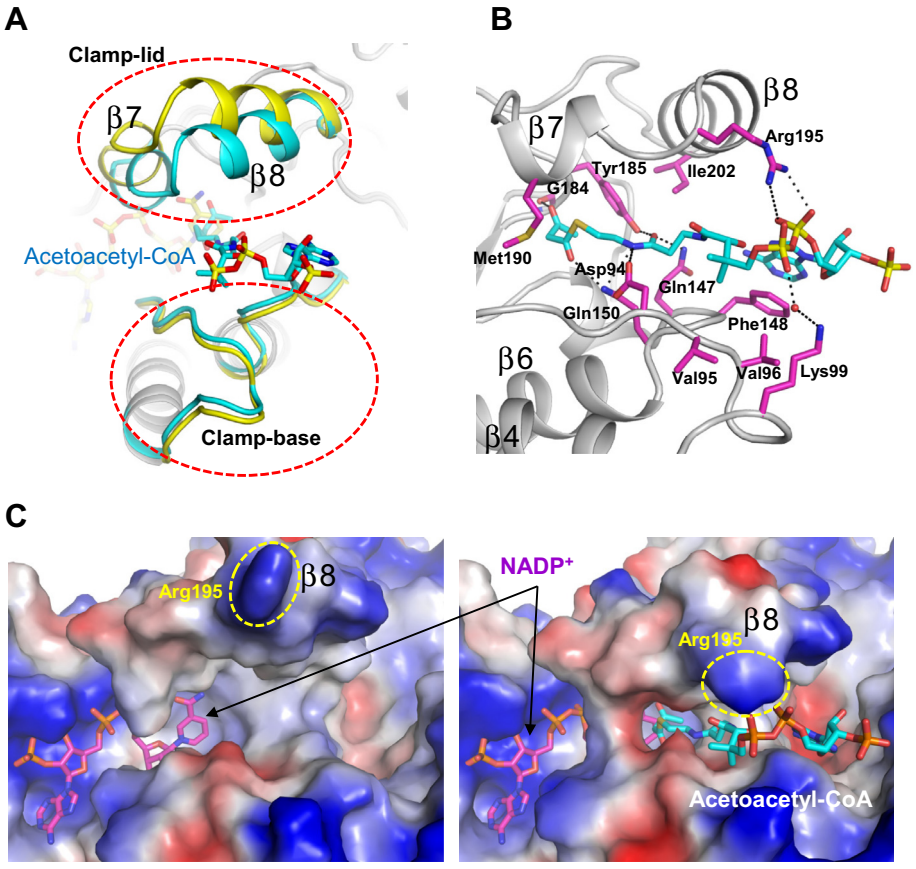

Fig. 3. Substrate binding mode of *Re*PhaB. (A) Conformational change of the Clamp domain. The Clamp-lid (α7 and α8) and the Clamp-base are distinguished with dashed red circles. The structures of acetoacetyl-CoA and $NADP^+$ bound *Re*PhaB were superposed, and presented as ribbon diagrams with cyan and yellow colors, respectively. The acetoacetyl-CoA is presented in the stick model with cyan color. (B) Stabilization of acetoacetyl-CoA. The bound acetoacetyl-CoA is presented in the stick model with cyan color. Residues involved in binding of the acetoacetyl-CoA are shown in the stick model with magenta color. Hydrogen bonds involved in the stabilization of the acetoacetyl-CoA were shown as black dotted-lines. The secondary structures are labeled appropriately. (C) Surface electrostatic presentation of the substrate binding site. *Re*PhaB structures without (left) and with (right) substrate binding are presented as surface electrostatic presentation with the same orientation. The arginine 195 residue in the α8 helix of the Clamp-lid is marked as yellow dashed circle, and labeled. The acetoacetyl-CoA and $NADP^+$ are shown as stick models with cyan and magenta colors, respectively. (For interpretation of the references to colour in this figure legend, the reader is referred to the web version of this article.)

It is clearly shown that acetoacetyl-CoA fits perfectly in the central cleft in the closed Clamp-lid conformation, but not in the open form (Fig. 3C). This suggests that the Clamp-lid is responsible for both recognition and stabilization of the substrate for catalysis.

3.4. Mutagenesis and biochemical analysis

Our structural data demonstrate that acetoacetyl-CoA binding to RePhaB is enabled by the conformational change of the Clamp domain. To test whether the interactions between acetoacetyl-CoA and key residues in the *Re*PhaB structure are biologically relevant, we performed series of mutagenesis and enzymatic activity assays. We picked seven residues around the Clamp domain that interact with acetoacetyl-CoA according to the complex structure, and changed to alanines (Fig. 3B). As we expected, enzymatic activity of all the mutants was lower than the wild type enzyme (Fig. 4). Four mutants (D94A, K99A, Y185A, and R195A) were almost completely inactivated, and the three mutants (Q147A, F148A and Q150A) showed 20~30% activity compared with the wild type. Our mutational analyses provide strong evidence for the substrate binding mechanism shown in our structure.

In summary, we determined the crystal structure of PhaB from *R. eutropha* H16, as the apoenzyme, in complex with the cofactor $NADP^+$, and in complex with the substrate acetoacetyl-CoA. The structure contains a Rossmann fold and a Clamp domain. The Rossmann fold has the same conformation in all three structures,

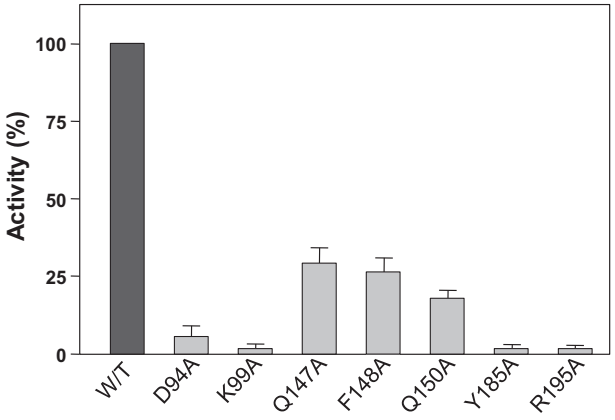

Fig. 4. Activity assays of the wild type and the mutant *Re*PhaB proteins. The acetoacetyl-CoA reductase activities of wild type and the mutant proteins were measured. The reaction mixture (1 ml) contained 100 mM MOPS, pH 7.0, 5 mM β-mercaptoethanol, 0.2 mM NADPH, and 0.2 mM acetoacetyl-CoA. For each reaction 1 μg of wild-type or mutant *Re*PhaB protein was added to start the reaction, and the decrease of absorbance at 340 nm was monitored at room temperature for 3 min. The error bars denote standard deviations from mean value of three independent reactions.

whereas the position of the Clamp domain is undergoes structural change upon substrate binding. Thus, we propose that the Clamp domain is involved in placing the substrate in the cleft and stabilizing the substrate conformation.

Acknowledgments

This work was supported by the Korea Research Foundation grant (313-2008-2-C00738) and the National Research Foundation of Korea Grant (NRF-2009-0072017) funded by the Korean Ministry of Education, Science, and Technology (MEST), and the Gyungbuk Sea Grant and the Marine Biotechnology Program funded by the Korean Ministry of Land, Transport and Maritime Affairs (MLTM).

References

[1] K. Sudesh, H. Abe, Y. Doi, Synthesis, structure and properties of polyhydroxyalkanoates: biological polyesters, Prog. Polym. Sci. 25 (2000) 1503–1555.
[2] W.N. He, Z.M. Zhang, P. Hu, C.Q. Chen, Microbial synthesis and characterization of polyhydroxyalkanoates by DG17 from glucose, Acta Polym. Sin. (1999) 709–714.
[3] A.J. Anderson, E.A. Dawes, Occurrence, metabolism, metabolic role, and industrial uses of bacterial polyhydroxyalkanoates, Microbiol. Rev. 54 (1990) 450–472.
[4] A. Steinbuchel, E. Hustede, M. Liebergesell, U. Pieper, A. Timm, H. Valentin, Molecular basis for biosynthesis and accumulation of polyhydroxyalkanoic acids in bacteria, FEMS Microbiol. Rev. 9 (1992) 217–230.
[5] X. Gao, J. Jian, W.J. Li, Y.C. Yang, X.W. Shen, Z.R. Sun, Q. Wu, G.Q. Chen, Genomic study of polyhydroxyalkanoates producing Aeromonas hydrophila 4AK4, Appl. Microbiol. Biotechnol. 97 (2013) 9099–9109.
[6] G.Q. Chen, A microbial polyhydroxyalkanoates (PHA) based bio- and materials industry, Chem. Soc. Rev. 38 (2009) 2434–2446.
[7] J. Jian, S.Q. Zhang, Z.Y. Shi, W. Wang, G.Q. Chen, Q. Wu, Production of polyhydroxyalkanoates by *Escherichia coli* mutants with defected mixed acid fermentation pathways, Appl. Microbiol. Biotechnol. 87 (2010) 2247–2256.
[8] T. Keshavarz, I. Roy, Polyhydroxyalkanoates: bioplastics with a green agenda, Curr. Opin. Microbiol. 13 (2010) 321–326.
[9] X. Gao, J.C. Chen, Q. Wu, G.Q. Chen, Polyhydroxyalkanoates as a source of chemicals, polymers, and biofuels, Curr. Opin. Biotechnol. 22 (2011) 768–774.
[10] L. Mauclaire, E. Brombacher, J.D. Bunger, M. Zinn, Factors controlling bacterial attachment and biofilm formation on medium-chain-length polyhydroxyalkanoates (Mcl-PHAs), Colloids Surf. B Biointerfaces 76 (2010) 104–111.
[11] S.Y. Lee, J.I. Choi, Production and degradation of polyhydroxyalkanoates in waste environment, Waste Manage. (Oxford) 19 (1999) 133–139.
[12] H. Ariffin, H. Nishida, M.A. Hassan, Y. Shirai, Chemical recycling of polyhydroxyalkanoates as a method towards sustainable development, Biotechnol. J. 5 (2010) 484–492.
[13] J.E. Kemnitzer, S.P. Mccarthy, R.A. Gross, Preparation of predominantly syndiotactic poly(beta-hydroxybutyrate) by the tributyltin methoxide catalyzed ring-opening polymerization of racemic beta-butyrolactone, Macromolecules 26 (1993) 1221–1229.
[14] E.N. Pederson, C.W. McChalicher, F. Srienc, Bacterial synthesis of PHA block copolymers, Biomacromolecules 7 (2006) 1904–1911.
[15] S. Ciesielski, J. Mozejko, G. Przybylek, The influence of nitrogen limitation on mcl-PHA synthesis by two newly isolated strains of Pseudomonas sp, J. Ind. Microbiol. Biotechnol. 37 (2010) 511–520.
[16] X. Han, Y. Satoh, T. Satoh, K. Matsumoto, T. Kakuchi, S. Taguchi, T. Dairi, M. Munekata, K. Tajima, Chemo-enzymatic synthesis of polyhydroxyalkanoate (PHA) incorporating 2-hydroxybutyrate by wild-type class I PHA synthase from *Ralstonia eutropha*, Appl. Microbiol. Biotechnol. 92 (2011) 509–517.
[17] T. Kichise, T. Fukui, Y. Yoshida, Y. Doi, Biosynthesis of polyhydroxyalkanoates (PHA) by recombinant *Ralstonia eutropha* and effects of PHA synthase activity on in vivo PHA biosynthesis, Int. J. Biol. Macromol. 25 (1999) 69–77.
[18] A. Pohlmann, W.F. Fricke, F. Reinecke, B. Kusian, H. Liesegang, R. Cramm, T. Eitinger, C. Ewering, M. Potter, E. Schwartz, A. Strittmatter, I. Voss, G. Gottschalk, A. Steinbuchel, B. Friedrich, B. Bowien, Genome sequence of the bioplastic-producing "Knallgas" bacterium *Ralstonia eutropha* H16, Nat. Biotechnol. 24 (2006) 1257–1262.
[19] B. Fuchtenbusch, A. Steinbuchel, Biosynthesis of polyhydroxyalkanoates from low-rank coal liquefaction products by *Pseudomonas oleovorans* and *Rhodococcus ruber*, Appl. Microbiol. Biotechnol. 52 (1999) 91–95.
[20] O.P. Peoples, A.J. Sinskey, Poly-beta-hydroxybutyrate (PHB) biosynthesis in *Alcaligenes eutrophus* H16. Identification and characterization of the PHB polymerase gene (phbC)), J. Biol. Chem. 264 (1989) 15298–15303.
[21] M. Shiraki, T. Endo, T. Saito, Fermentative production of (R)-(-)-3-hydroxybutyrate using 3-hydroxybutyrate dehydrogenase null mutant of *Ralstonia eutropha* and recombinant *Escherichia coli*, J. Biosci. Bioeng. 102 (2006) 529–534.
[22] T. Kichise, S. Taguchi, Y. Doi, Enhanced accumulation and changed monomer composition in polyhydroxyalkanoate (PHA) copolyester by in vitro evolution of Aeromonas caviae PHA synthase, Appl. Environ. Microbiol. 68 (2002) 2411–2419.
[23] B. Bowien, B. Kusian, Genetics and control of CO(2) assimilation in the chemoautotroph *Ralstonia eutropha*, Arch. Microbiol. 178 (2002) 85–93.
[24] Z. Otwinowski, W. Minor, Processing of X-ray diffraction data collected in oscillation mode, Macromol. Crystallogr. Pt A 276 (1997) 307–326.
[25] A. Vagin, A. Teplyakov, Molecular replacement with MOLREP, Acta Crystallogr. D Biol. Crystallogr. 66 (2010) 22–25.
[26] P. Emsley, K. Cowtan, Coot: model-building tools for molecular graphics, Acta Crystallogr. D 60 (2004) 2126–2132.
[27] G.N. Murshudov, A.A. Vagin, E.J. Dodson, Refinement of macromolecular structures by the maximum-likelihood method, Acta Crystallogr. D 53 (1997) 240–255.
[28] A.T. Brunger, P.D. Adams, G.M. Clore, W.L. DeLano, P. Gros, R.W. Grosse-Kunstleve, J.S. Jiang, J. Kuszewski, M. Nilges, N.S. Pannu, R.J. Read, L.M. Rice, T. Simonson, G.L. Warren, Crystallography & NMR system: a new software suite for macromolecular structure determination, Acta Crystallogr. D 54 (1998) 905–921.
[29] A.C. Price, Y.M. Zhang, C.O. Rock, S.W. White, Cofactor-induced conformational rearrangements establish a catalytically competent active site and a proton relay conduit in FabG, Structure 12 (2004) 417–428.